scientific reports

Check for updates

OPEN

Feasibility of multisource CBCT for improving the predictability of dental implant primary stability compared to conventional CBCT

Wei Luo[1], Yuanming Hu[1], Amanda Finger Stadler[2], Antonio J. Moretti[2], Donald A. Tyndall[3], Christina R. Inscoe[1], Yueh Z. Lee[4], Jianping Lu[1] & Otto Zhou[1]✉

Cone beam computed tomography (CBCT) is the current 3D imaging modality of choice in dentistry and is widely used for presurgical implant planning. Implant sites can potentially be evaluated based on their CBCT-derived Hounsfield Units (HU) values, from which clinical decisions, including suitability for implant placement and surgical approach can be made. The current CBCT, however, is inaccurate and unreliable for quantifying the HU, and attempts to correlate CBCT-derived HU with implant primary stability have produced mixed results. This study demonstrated that the novel multisource CBCT (ms-CBCT) enabled by the distributed carbon nanotube (CNT) x-ray source array technology provides a stronger correlation between the cortical bone density of porcine femur approximated by the HU values and the implant primary stability measured by the implant insertion torque, when compared to the conventional single-source CBCT. Twelve planned dental implant sites were imaged with both ms-CBCT and conventional CBCT. The averaged bone HU value was obtained around each site, and insertion torque was measured intraoperatively. Linear regression demonstrated a strong and statistically significant correlation between insertion torque and ms-CBCT-derived HU ($R^2 = 0.86$, $p = 0.00014$), while conventional CBCT showed a weaker but still significant correlation ($R^2 = 0.55$, $p = 0.0056$). These findings suggest that by mitigating x-ray photon scatter and cone beam artifacts, the ms-CBCT derived HU better reflects local bone quality relevant to implant stability, highlighting its potential to improve patient-specific implant planning and improve overall dental implant success.

Abbreviations

CBCT-1	The ms-CBCT operating in the conventional CBCT configurationa, with a single source at a wide cone angle to cover the entire FOV
ms-CBCT	Multisource Cone Beam Computed Tomography
GV	Greyscale Value
HU	CT Hounsfield Unit

Dental implants have revolutionized dental treatment by providing an effective solution for replacing missing teeth and restoring oral function and aesthetics[1]. One study estimated the implant prevalence among adults missing at least one tooth in the U.S. was 5.7% in 2016 and could reach up to 23% by 2026[2]. Long term success of implants requires, among many factors, mechanical (primary) stability, which is strongly influenced by local bone quality and quantity[1–3], to facilitate implant osseointegration with the surrounding bone structure[1]. Bone mineral density (BMD) is used clinically to evaluate the bone quality prior to surgery, to select a suitable implant site and to predict the primary stability[3–5]. Low BMD often results in low primary stability and delays on the final prosthetic rehabilitation.

Volumetric BMD can be determined by quantitative computed tomography (qCT)[6] and dual energy CT (DECT)[7], or assessed directly using the CT Hounsfield Unit (HU) value which scales with the BMD. Several studies have shown that there is a statistically significant correlation between the BMD/HU and the implant

[1]Department of Physics and Astronomy, University of North Carolina at Chapel Hill, Chapel Hill, NC 27599, USA. [2]Department of Periodontology, Endodontics and Dental Hygiene, Adams School of Dentistry, University of North Carolina at Chapel Hill, Chapel Hill, NC 27599, USA. [3]Department of Diagnostic Sciences, Adams School of Dentistry, University of North Carolina at Chapel Hill, Chapel Hill, NC 27599, USA. [4]Department of Radiology, School of Medicine, University of North Carolina at Chapel Hill, Chapel Hill, NC 27599, USA. ✉email: zhou@email.unc.edu

primary stability estimated by the insertion torque value (ITV) for implant placement[5,8–10]. However, CT, in general, requires high radiation exposure, high cost and large footprint and is not accessible for most dental clinics. Cone beam CT (CBCT) is the current 3D imaging modality of choice in dentistry[11,12] and is used in presurgical dental implant planning[13]. Potential implant sites are evaluated based on their CBCT derived HU and are stratified into several categories following, for example, the Misch classification[14], based on which clinical decisions including suitability for implant placement and surgical approach are made.

The current CBCT, however, is highly inaccurate and unreliable for quantifying the HU, with errors in the order of several hundred HU's[15-17]. This has been attributed to the presence of strong x-ray photon scatter, beam hardening and incomplete data sampling that are intrinsic to the current CBCT design. Many commercial CBCT scanners provide only the image Grayscale Value (GV) instead of the HU. A recent study of two clinical CBCT units using multiple commercial implant planning software concluded that it was not possible to measure the HU reliably due to its large variations[18]. Attempts to correlate CBCT-derived HU/GV with implant primary stability produced mixed results varying from no[19], weak[20,21], to strong[22] correlations. The inaccuracy leads to mischaracterization of bone types, unreliable prediction of implant stability, potentially incorrect clinical decisions, and an increased risk of implant failure.

The motivation of this study was to evaluate whether the accuracy of predicting implant primary stability can be improved by evaluating the BMD using a new multisource CBCT (ms-CBCT)[23,24], which was designed with the aim to overcome the intrinsic limitations of the current CBCT. It replaces the conventional single wide cone angle x-ray tube with a carbon nanotube (CNT) based field emission x-ray source array[25,26] that generates a stack of narrowly collimated x-ray beams[23,27,28]. Phantom imaging studies have shown the ms-CBCT significantly improves the HU accuracy, enhances the soft tissue contrast resolution, and reduces cone beam artifacts without increasing the radiation exposure, compared to multiple clinical dental CBCT scanners[23,27,29]. In this study, the relation between the ms-CBCT derived HU and the ITV for placing dental implants to porcine femurs was evaluated and compared to that of a CBCT. The results show a statistically significant correlation between the ms-CBCT derived HU and the ITV and a weak correlation between the conventional CBCT derived HU and the ITV.

Materials and methods

Specimen Preparation

Four commercially obtained frozen porcine femurs (from My Pet Carnivore, Indianapolis, IN 46201) were prepared for implant placement by first cleaning the surface soft tissue along the mid-femoral region. The femurs were initially stored at − 20 °C, then thawed at room temperature for 12–24 h prior to implant placement. Twelve identical titanium dental implants (NobelActive NP, 3.5 × 10 mm, Nobel Biocare) was utilized across the femurs to ensure consistency. The osteotomy for each implant site was prepared in stages, with sequential drilling from a precision drill (∅ ≈ 1.5 mm) to identify the entry point on the cortical surface and confirm appropriate alignment with the femur's long axis. Drilling diameters were then increased gradually following the manufacturer's guidelines until the ∅3.2 mm twist drill. The implant was inserted with a hand piece at a consistent speed and angulation maintained uniformly across all trials. Each femur accommodated three distinct osteotomy sites in the mid-diaphyseal cortical region, spaced at least 1 cm apart, to reduce the chance of structural overlap or bone weakening from previous placements. IACUC approval was not required because this study did not involve living vertebrate animals.

Implant primary stability test

The maximum insertion torque value (ITV) for placing an implant, a commonly used technique to evaluate the implant mechanical stability, was recorded as each implant was placed into its prepared osteotomy. A digital torque wrench (Vpoer Digital Torque Wrench 1/4-inch Drive) equipped with a compatible implant driver was set to peak mode to capture the highest torque value attained during insertion. The wrench's threshold was configured to not exceed the expected maximum torque. Implants were aligned with the osteotomy and inserted in a clockwise direction at a consistent speed until stopped. The maximal ITV displayed on the wrench was taken as the outcome measurement. The implant placement procedure is shown in Fig. 1.

Imaging using ms-CBCT and CBCT

The benchtop ms-CBCT scanner[23] consists of a CNT x-ray source array (NuRay Technologies, ChangZhou, China) and a flat panel detector (Xineos-1511, Teledyne, CA) on a rotating gantry, as illustrated in Fig. 2. The system geometry is similar to that of a commercial dental CBCT[30] (CS9300, Carestream Dental, USA). The x-ray source array contains 8 focal spots ("sources") with a 12 mm inter-spot spacing, each with the output power and the spatial resolution of a typical fixed-anode dental x-ray tube[30]. The radiation from each focal spot is confined to a narrow cone angle by an external multisource collimator to expose only a small section of the object in the axial direction and the full detector width. The 8 collimated beams collectively cover the entire FOV. They are activated sequentially to cycle 361 times in one full gantry rotation, producing 2880 image frames.

To avoid complications from other factors such as variations in the system configuration, exposure parameters, and the reconstruction method, the ms-CBCT was compared to the same benchtop device operating in the conventional CBCT configuration using only one of the eight CNT x-ray sources and a separate wide cone-angle collimator under otherwise the same imaging conditions (referred to as "CBCT-1"). The benchtop ms-CBCT system is shown in Fig. 2. Previous studies have shown the imaging performance of CBCT-1 is similar to the clinical dental CBCT scanners investigated[23,29]. The femur bone with the implants was placed inside a cylindrical plastic container filled with water to simulate scatter from soft tissue. The exposure parameters used by the two scanners are shown in Table 1, which are similar to those used for CBCT imaging of an adult patient under the standard protocol in our institution.

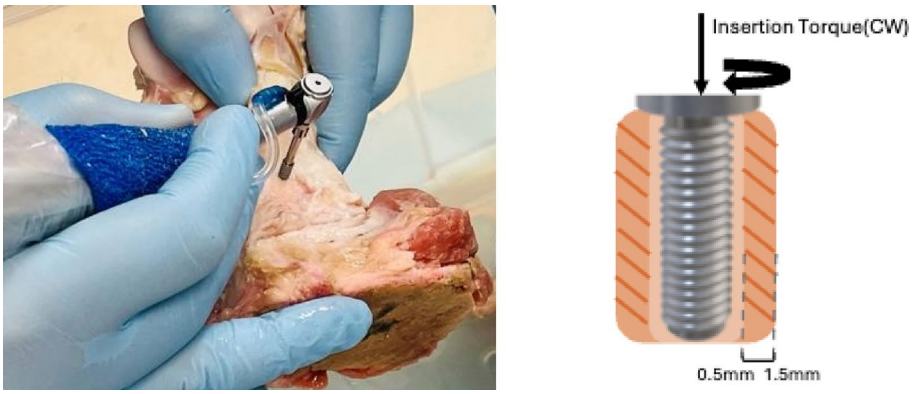

Fig. 1. Titanium dental implant was placed into a porcine femur bone following manufacture recommended procedure. The maximum insertion torque value (ITV) for placing the implant was recorded.

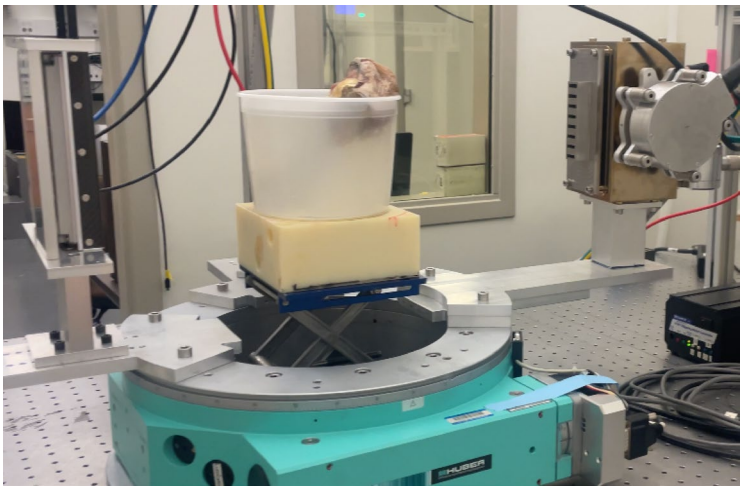

Fig. 2. A photo of the benchtop ms-CBCT with a CNT x-ray source array and a multisource collimator that generates a stack of narrowly collimated x-ray beams in the axial direction.

	ms-CBCT	CBCT-1
Number of X-ray sources	**8**	**1**
X-ray voltage (kV)	110	110
X-ray current (mA)	11	11
Filtration	0.3 mm Cu + 1.7 mm Al	0.3 mm Cu + 1.7 mm Al
Exposure time per proj. (ms)	5	5
Total x-ray exposure (mAs)	19.80	19.80
FOV (cm x cm)	18.7 × 10	18.7 × 7.4

Table 1. Imaging protocols of the ms-CBCT and CBCT-1.

Image reconstruction and analysis

The projection images from the ms-CBCT were first processed using an adjacent scatter ratio subtraction (ASRS) method enabled by this imaging configuration[27]. The processed projections from all sources were then used for volumetric CT reconstruction using the 3D Simultaneous Iterative Reconstruction Technique (SIRT) algorithm based on the ASTRA Toolbox[31]. The reconstruction was performed using a single system matrix, including the source/detector rays from all sources[23]. The total variation (TV) algorithm was incorporated for image noise reduction based on the Tigre Toolbox[32,33]. The CT numbers of all reconstructions were calibrated according to Gammex CT ACR 464 phantom (Sun Nuclear) testing instruction. The projection images from CBCT-1 were reconstructed using the same algorithm without ASRS processing. Reconstructions were generated using voxel sizes of 0.25 mm × 0.25 mm × 0.25 mm.

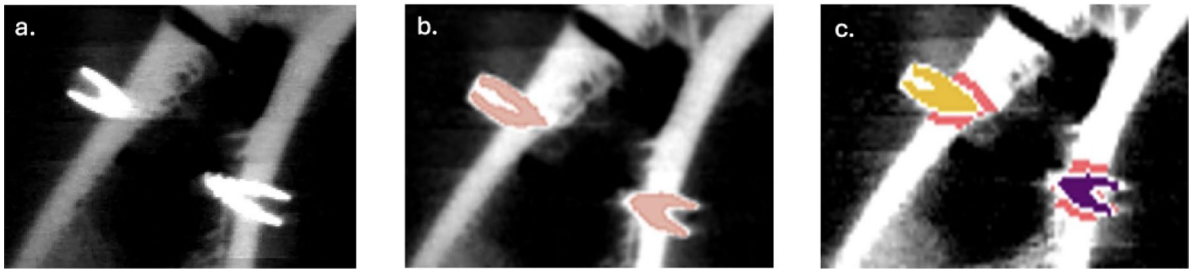

Fig. 3. A reconstructed ms-CBCT image showing two implants after **(a)** reconstruction, **(b)** segmentation, and **(c)** identifying the annular peri-implant bone regions (in red color). The clear hole through the cortical bone is the result from a failed implant placement where the implant was drilled through the bone.

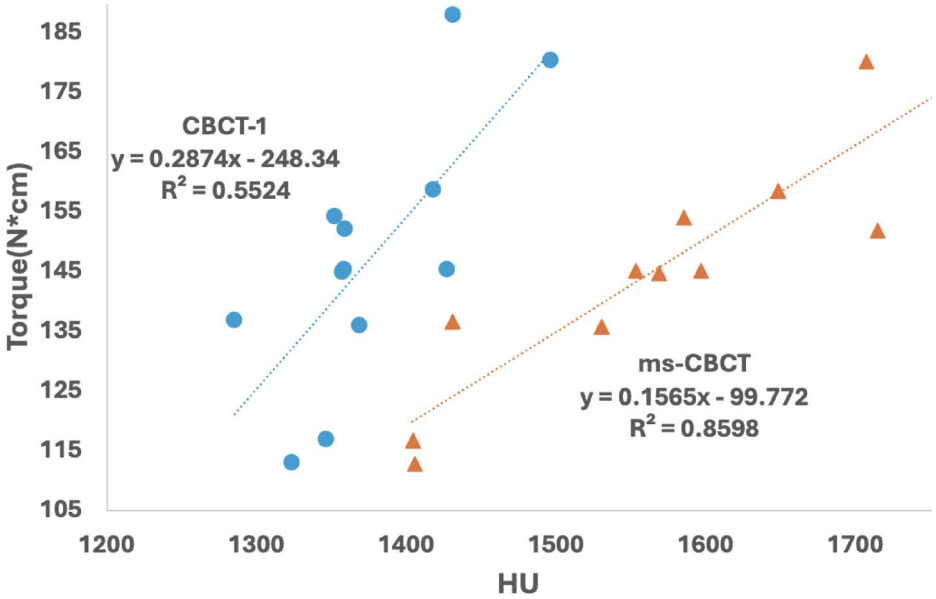

Fig. 4. A scatter plot of insertion torque value against measured cortical bone HU. Although the dataset is modest in size, the ms-CBCT regression curve yields a stronger coefficient of determination ($R^2 \approx 0.86$) compared to the CBCT-1 ($R^2 \approx 0.55$).

The reconstructed dataset underwent additional processing to facilitate implant segmentation and peri-implant bone density assessment. First, the reconstructed volume was imported into the 3D Slicer software[34] (version 5.6.1). A threshold of 2400 HU was applied to segment the titanium implant from the surrounding bone structure. A custom script was then used to identify the implant volume in the segmentation using connected-component labelling. The script also defined an annular bone region surrounding the implant, with an inner and outer surface respectively 0.5 mm and 1.5 mm away from the implant surface, as illustrated in Fig. 1. The mean HU value within this annulus volume was computed. Any voxels with the CT numbers < 1000 HU were excluded in the calculation to eliminate the trabecular bones and soft tissues, leaving only higher-density cortical bone for analysis. This procedure was repeated for each implant and for both the ms-CBCT and CBCT-1 scans, ensuring consistency in the ROI selection and HU computation. The thickness of the cortical bone supporting the implants was also measured using the Line tool in ImageJ by drawing a straight line across the cortical region, and the displayed length was recorded.

The mean HU values extracted from each peri-implant region were correlated with the corresponding ITV's recorded during implant placement. A linear regression was performed for the data from each scanner, and the coefficient of determination (R^2) was calculated to quantify the strength of each correlation.

Results

Figure 3. shows an example of the reconstructed ms-CBCT image of a femur with two implants. The implant volumes determined from segmentation and the annular shells used to compute the averaged peri-implant bone densities are displayed in Fig. 3b) and Fig. 3c), respectively.

Figure 4 shows the measured maximum ITV versus the averaged HU of the cortical bones derived from the ms-CBCT (triangle) and a CBCT-1 (circle). Each dataset consists of data from two femur bones. The solid lines

are results from linear regression analysis. A positive strong correlation is observed between the ITV and ms-CBCT derived HU, with ITV (N×cm) = 0.1565 × HU – 99.772. The coefficient of determinant R^2 is 0.86 and the calculated p-value is 0.00014 indicating a statistically significant correlation between the ITV and the HU. For the HU value derived from CBCT-1, linear regression shows a weak correlation of ITV (N×cm) = 0.2844 × HU – 248.32, with a R^2 of 0.55 and a p-value of 0.0056.

Discussion

The results from this study show there is a statistically significant correlation (R^2 = 0.86, P = 0.00015) between the ms-CBCT derived cortical bone HU and the implant primary stability measured by its maximum insertion torque value. This is consistent with the conclusions from prior studies using CT and qCT[5,8–10], and is a significant improvement compared to the conventional CBCT, which shows only a weak correlation in this study and mixed results in previous reports[19–22]. Contrary to a previous report using a conventional CBCT and porcine ilium model[22], the result from this study shows no correlation between the cortical bone thickness and the ITV.

In an experiment using limited number of postmortem mandibles and a qCT, Homolka et al. found a strong correlation (R^2 = 0.83 and $P < 0.001$) between the BMD and the implant ITV. Similarly, Ikumi and coworkers reported a strong correlation between CT derived HU values and the implant ITV (R^2 = 0.77) in a pilot patient study[9]. In contrast, results from prior publications using CBCT are inconclusive. A study using porcine mandibular condyles and CBCT reported statistically insignificant correlation[19]. A low correlation was found for placing implants into the patient maxilla (r = 0.329)[20]. One study using pig ilium by Wada and coworkers showed a positive correlation (R^2 = 0.63)[22]. Recently, Vautrin et al. reported that there was a weak correlation in an experiment using cadaveric mandibles (R^2 = 0.39) and showed the correlation was improved by further finite element analysis[21]. The result obtained from the conventional CBCT-1 in this study (R^2 = 0.55) is within the range of those from previously publications using CBCT.

The large variation and overall weak correlation between the BMD derived from the conventional CBCT and implant primary stability are attributed to the intrinsic limitations of the current CBCT design. They are known to be inaccurate and inconsistent in quantifying the HU. The presence of strong scatter from the large imaging volume causes underestimation of the linear attenuation coefficient and consequently the HU value. This is clearly shown in Fig. 4, where the HU value calculated from CBCT-1 is ~ 100–200 HU smaller than that from the ms-CBCT for the same ROI. In addition, for the same material, CBCT derived HU varies with position inside the object due to scatter and beam hardening, which is known as the "Cupping" artifact. The image quality and accuracy are further compromised by the presence of cone beam artifacts caused by the large divergency of the x-ray beams and the resulting undersampling in regions away from the central imaging plane. The HU values are also strongly affected by imaging protocol including the field of view[16]. As a result, CBCT derived HU/GV is not a reliable measure of the bone density/quality and cannot reliably predict the implant primary stability.

There has been considerable amount of research directed towards improving the accuracy of dental CBCT for quantifying HU/BMD[16], primarily through software-based postprocessing[35,36]. The ms-CBCT was designed to overcome the root cause problem of the current clinical CBCT, the large imaging volume, by replacing the wide cone angle x-ray tube with multiple narrow cone angle x-ray beams (2.4 degrees per beam vs. 10.5 degrees in CBCT-1)[23,27]. This significantly reduces scatter and cone-beam artifact and consequently improves the HU accuracy. A study comparing the HU accuracy of the ms-CBCT and several clinical CBCT[23] units reports that the median deviation from the clinical CT was reduced from – 166.7HU and 354.4 HU for the two clinical CBCT units (Accuitomo 170 from J. Morita and CS9300 from Carestream Dental) to 43.7HU for the ms-CBCT in the Bland-Altman analysis. A separate study reports the ms-CBCT improves the accuracy of jawbone BMD compared to the two commercial CBCT scanners evaluated[29]. The enhanced HU accuracy and reliability contribute to the improved correlation between the ms-CBCT derived HU and the implant ITV observed in this study.

This feasibility study has its limitations. The scope of this study was limited. Only twelve implants of the same diameter and length were evaluated. A larger size sample that also includes implants with different specifications would be more desirable and will be used in follow up studies to improve the statistics and to cover the different clinical scenarios. Porcine femurs instead of mandibles were tested because of their consistent availability and comparable bone structure. Their cortical bones have higher HU and ITV values when compared to those from a typical human jawbone. The range of the HU values of their cortical bones is relatively narrow and does not cover the entire range of the different grades of bones in the Misch classification. This is not expected to change the conclusion of this report but needs to be validated in future studies. In a previous study, for example, we show the ms-CBCT is significantly more accurate than CBCT-1 in measuring the HU value of a dried human skull for both cortical and cancellous bones in the entire range of 0-2000HU[29]. Multiple implants were placed in each femur. The metal artifacts caused by the implants in proximity could affect the HU values of cortical bones.

The new ms-CBCT improves the imaging performance without increasing the imaging Air Kerma compared to a conventional CBCT. In this study, the Air Kerma value for the ms-CBCT is slightly lower than that of a conventional CBCT (NT5G, New Tom, Italy) in the normal dose protocol for an adult patient in our institution. The ms-CBCT scanner with multiple narrowly collimated x-ray beams acquires more image frames and requires a faster detector readout to maintain the scanning time compared to a conventional CBCT. By replacing the half-width and laterally offset FPD used presently with a full width one and by utilizing region of interest readout to reduce the detector readout time, an estimated scanning time of ~ 12 s can be achieved, which is within the range of the current dental CBCT with a similar FOV[17,30]. The ms-CBCT technology is still in the development stage. The main cost difference between this and a conventional CBCT is the CNT x-ray source array. Based on the costs of the multisource CNT x-ray source array manufactured for an intraoral tomosynthesis device[37] and the monoblock x-ray generator used in the conventional CBCT, the cost of the ms-CBCT will be slightly higher

but not significantly. The device can be constructed by retrofitting a conventional CBCT with the CNT x-ray source array.

Conclusion

This preliminary study demonstrates an improved correlation between the Hounsfield Unit value measured from the new ms-CBCT and the maximum implant insertion torque, suggesting that the ms-CBCT technology can improve the accuracy and reliability of predicting implant stability in presurgical dental implant planning compared to the current clinical CBCT.

Data availability

The datasets used and/or analyzed during the current study are available from the corresponding author on reasonable request.

Received: 8 September 2025; Accepted: 4 February 2026
Published online: 07 February 2026

References

1. Buser, D., Sennerby, L. & De Bruyn, H. Modern implant dentistry based on osseointegration: 50 years of progress, current trends and open questions. *Periodontol 2000*. **73**, 7–21. https://doi.org/10.1111/prd.12185 (2017).
2. Elani, H. W., Starr, J. R., Silva, D., Gallucci, G. O. & J. D. & Trends in dental implant use in the U.S., 1999–2016, and projections to 2026. *J. Dent. Res.* **97**, 1424–1430. https://doi.org/10.1177/0022034518792567 (2018).
3. Kopperdahl, D. L., Morgan, E. F. & Keaveny, T. M. Quantitative computed tomography estimates of the mechanical properties of human vertebral trabecular bone. *J. Orthop. Res.* **20**, 801–805. https://doi.org/10.1016/S0736-0266(01)00185-1 (2002).
4. Molly, L. Bone density and primary stability in implant therapy. *Clin. Oral Implants Res.* **17** (Suppl 2), 124–135. https://doi.org/10.1111/j.1600-0501.2006.01356.x (2006).
5. Turkyilmaz, I. & McGlumphy, E. A. Influence of bone density on implant stability parameters and implant success: a retrospective clinical study. *BMC Oral Health*. **8**, 32. https://doi.org/10.1186/1472-6831-8-32 (2008).
6. Adams, J. E. Quantitative computed tomography. *Eur. J. Radiol.* **71**, 415–424. https://doi.org/10.1016/j.ejrad.2009.04.074 (2009).
7. Koch, V. et al. Accuracy and precision of volumetric bone mineral density assessment using dual-source dual-energy versus quantitative CT: a Phantom study. *Eur. Radiol. Exp.* **5**, 43. https://doi.org/10.1186/s41747-021-00241-1 (2021).
8. Homolka, P. et al. Bone mineral density measurement with dental quantitative CT prior to dental implant placement in cadaver mandibles: pilot study. *Radiology* **224**, 247–252. https://doi.org/10.1148/radiol.2241010948 (2002).
9. Ikumi, N. & Tsutsumi, S. Assessment of correlation between computerized tomography values of the bone and cutting torque values at implant placement: a clinical study. *Int. J. Oral Maxillofac. Implants*. **20** (2), 253–260 (2005).
10. Kim, J. H., Lim, Y. J., Kim, B. & Lee, J. How do parameters of implant primary stability correspond with CT-Evaluated bone quality in the posterior maxilla? A correlation analysis. *Mater. (Basel)*. 14. https://doi.org/10.3390/ma14020270 (2021).
11. Scarfe, W. C. & Angelopoulos, C. *Maxillofacial Cone Beam Computed Tomography*. (2018).
12. Gaêta-Araujo, H. et al. Cone beam computed tomography in dentomaxillofacial radiology: a two-decade overview. *Dentomaxillofac Radiol.* **49**, 20200145. https://doi.org/10.1259/dmfr.20200145 (2020).
13. Jacobs, R., Salmon, B., Codari, M., Hassan, B. & Bornstein, M. M. Cone beam computed tomography in implant dentistry: recommendations for clinical use. *BMC Oral Health*. **18**, 88. https://doi.org/10.1186/s12903-018-0523-5 (2018).
14. Misch, C. E. Density of bone: effect on treatment plans, surgical approach, healing, and progressive Boen loading. *Int. J. Oral Implantol.* **6**, 23–31 (1990).
15. Siewerdsen, J. H. & Jaffray, D. A. Cone-beam computed tomography with a flat-panel imager: magnitude and effects of x-ray scatter. *Med. Phys.* **28**, 220–231. https://doi.org/10.1118/1.1339879 (2001).
16. Pauwels, R., Jacobs, R., Singer, S. R. & Mupparapu, M. CBCT-based bone quality assessment: are Hounsfield units applicable? *Dentomaxillofac Radiol.* **44**, 20140238. https://doi.org/10.1259/dmfr.20140238 (2015).
17. Kaasalainen, T., Ekholm, M., Siiskonen, T. & Kortesniemi, M. Dental cone beam CT: an updated review. *Phys. Med.* **88**, 193–217. https://doi.org/10.1016/j.ejmp.2021.07.007 (2021).
18. Nagata, K. et al. Accuracy of the Hounsfield unit values measured by implant planning software. *Dent. J. (Basel)*. **12** https://doi.org/10.3390/dj12120413 (2024).
19. Lee, S. H. et al. Low bone density predictability of CBCT and its relation to primary stability of tapered implant design: A pilot study. *J. Oral Implantol.* **49**, 556–563. https://doi.org/10.1563/aaid-joi-D-21-00159 (2023).
20. Hakim, S. G., Glanz, J., Ofer, M., Steller, D. & Sieg, P. Correlation of cone beam CT-derived bone density parameters with primary implant stability assessed by peak insertion torque and Periotest in the maxilla. *J. Craniomaxillofac. Surg.* **47**, 461–467. https://doi.org/10.1016/j.jcms.2019.01.002 (2019).
21. Vautrin, A. et al. Prediction of dental implants primary stability with cone beam computed Tomography-Based homogenized finite element analysis. *Clin. Implant Dent. Relat. Res.* **27**, e70016. https://doi.org/10.1111/cid.70016 (2025).
22. Wada, M. et al. The relationship between the bone characters obtained by CBCT and primary stability of the implants. *Int. J. Implant Dent.* **1**, 3. https://doi.org/10.1186/s40729-014-0003-x (2015).
23. Xu, S. et al. Volumetric computed tomography with carbon nanotube X-ray source array for improved image quality and accuracy. *Commun. Eng.* **2** https://doi.org/10.1038/s44172-023-00123-x (2023).
24. Tyndall, D. A., Price, J. B., Gaalaas, L. & Spin-Neto, R. Surveying the landscape of diagnostic imaging in dentistry's future: four emerging technologies with promise. *J. Am. Dent. Assoc.* **155**, 364–378. https://doi.org/10.1016/j.adaj.2024.01.005 (2024).
25. Christina Inscoe, Y. Z. L. & Lu, J. Otto Zhou. in Nanostructured Carbon Electron Emitters and Applications (ed Saito, Y.) (Jenny Stanford Publishing Pte Ltd, (2020).
26. Zhang, J. et al. Stationary scanning x-ray source based on carbon nanotube field emitters. *Appl. Phys. Lett.* **86** https://doi.org/10.1063/1.1923750 (2005).
27. Xu, S. et al. Evaluation of the feasibility of a multisource CBCT for maxillofacial imaging. *Phys. Med. Biol.* **68** https://doi.org/10.1088/1361-6560/acea17 (2023).
28. Li, B. et al. A carbon nanotube x-ray source array designed for a new multisource cone beam computed tomography scanner. *Phys. Med. Biol.* **69** https://doi.org/10.1088/1361-6560/ad3323 (2024).
29. Hu, Y. et al. Improving the accuracy of bone mineral density using a multisource CBCT. *Sci. Rep.* **14**, 3887. https://doi.org/10.1038/s41598-024-54529-4 (2024).
30. Ludlow, J. B. et al. Effective dose of dental CBCT-a meta analysis of published data and additional data for nine CBCT units. *Dentomaxillofac Radiol.* **44**, 20140197. https://doi.org/10.1259/dmfr.20140197 (2015).
31. van Aarle, W. et al. The ASTRA toolbox: A platform for advanced algorithm development in electron tomography. *Ultramicroscopy* **157**, 35–47. https://doi.org/10.1016/j.ultramic.2015.05.002 (2015).

32. Sidky, E. Y. & Pan, X. Image reconstruction in circular cone-beam computed tomography by constrained, total-variation minimization. *Phys. Med. Biol.* **53**, 4777–4807. https://doi.org/10.1088/0031-9155/53/17/021 (2008).
33. Biguri, A., Dosanjh, M., Hancock, S. & Soleimani, M. TIGRE: a MATLAB-GPU toolbox for CBCT image reconstruction. *Biomedical Phys. Eng. Express*. **2** https://doi.org/10.1088/2057-1976/2/5/055010 (2016).
34. Fedorov, A. et al. 3D slicer as an image computing platform for the quantitative imaging network. *Magn. Reson. Imaging*. **30**, 1323–1341. https://doi.org/10.1016/j.mri.2012.05.001 (2012).
35. Yong, T. H. et al. QCBCT-NET for direct measurement of bone mineral density from quantitative cone-beam CT: a human skull Phantom study. *Sci. Rep.* **11**, 15083. https://doi.org/10.1038/s41598-021-94359-2 (2021).
36. Park, C. S. et al. Validation of bone mineral density measurement using quantitative CBCT image based on deep learning. *Sci. Rep.* **13**, 11921. https://doi.org/10.1038/s41598-023-38943-8 (2023).
37. Inscoe, C. R. et al. Characterization and preliminary imaging evaluation of a clinical prototype stationary intraoral tomosynthesis system. *Med. Phys.* **45**, 5172–5185 (2018).

Author contributions

W.L. contributed to the experimental setup, participated in the data acquisition, performed image reconstructions, performed torque measurements, carried out data analysis, and wrote the original draft. Y.H. contributed to the experimental setup, participated in the data acquisition. C.R.I. contributed to the experimental setup, characterized the CNT source array, and supervised the whole work. A.S. and A.M. assisted with implant placement, bone quality assessment, and provided clinical advising. D.A.T. supervised the whole work and represented the perspective of a dentist and maxillofacial radiologist. Y.Z.L. supervised the whole work. J.L. conceived the concept of the ms-CBCT and supervised the whole work. O.Z. conceived the concept of the ms-CBCT, supervised the whole work, and wrote the original draft. All authors were involved in revising the manuscript.

Funding

This work was supported in part by the National Institutes of Health (NIH) under grant R56DE030962-01.

Declarations

Competing interests

The authors declare the following competing interests: O.Z. has equity ownership and serves on the board of directors of XinVisio, LLC., to which the technologies used or evaluated in this project have been licensed, and NuRay Co., Ltd, which manufactures the x-ray sources used in this study. J.L. has equity ownership in XinVisio, LLC. and NuRay Co. Ltd. O.Z., J.L., C.R.I., Y.Z.L., and B.L. are co-inventors of licensed technology evaluated in this study. All activities have been approved by the institutional COI committee. All other authors declare no competing interests.

Additional information

Correspondence and requests for materials should be addressed to O.Z.